Global Downstream River Flows and Continental Runoff: An Update to 2024

AIGUO DAI,[a] JUN HU,[c] ANMIN DUAN,[b,c] XIANGHUI GUO,[b] MING LIU,[b,c] RISHENG LIANG,[b,c] GUIZHI WANG,[b] AND MINHAN DAI[b]

[a] *Department of Atmospheric and Environmental Sciences, University at Albany, State University of New York, Albany, New York*
[b] *State Key Laboratory of Marine Environmental Science and College of Ocean and Earth Sciences, Xiamen University, Xiamen, China*
[c] *Center for Marine Meteorology and Climate Change, College of Ocean and Earth Sciences, Xiamen University, Xiamen, China*

(Manuscript received 14 January 2026, in final form 18 May 2026, accepted 16 September 2026)

ABSTRACT: Monitoring continental runoff is important for the global water cycle. Here, we update downstream monthly streamflow for the world's 936 largest rivers to 2024 using multiple data sources for quantifying variations and long-term changes in continental discharge from 1950 to 2024. The update added new data for 697 rivers and extended the record length for 512 rivers. Still, many large rivers in South and East Asia, Africa, and some in South America have short records, and stations with observations have decreased since 1978. Streamflow in the world's major rivers exhibits large interannual-to-decadal variations that are correlated with basin-mean precipitation, with insignificant long-term trends since 1948 for most of the rivers. Out of the 200 rivers with the largest discharges, only 71 (35.5%) show statistically significant streamflow trends during 1948–2024, with 34 being positive and 37 being negative. Global continental discharge decreased slightly from 1949 to 1993 and then rebounded to levels slightly above the 1950–90 mean in recent years. The streamflow-inferred runoff trends during 1950–2024 show coherent spatial patterns that are broadly consistent with observed precipitation trends, both showing increases over the central and Northeast United States, northern Europe and most of Russia, Argentina and Uruguay, and northwestern Australia, but decreases over most of Africa, East and South Asia, eastern Australia, the western United States, western and eastern Canada, and parts of Brazil. Both internal climate variability (especially from the tropical Pacific) and externally forced changes [e.g., due to carbon dioxide (CO_2) increases] likely contributed to these regional trends in precipitation and runoff, with below (above)-normal land precipitation and runoff during warm (cold) phases of the tropical Pacific sea surface temperatures.

KEYWORDS: Climate variability; Interannual variability; Trends; Hydrologic cycle; Rivers; Runoff

1. Introduction

During a rainstorm or a snowmelt event, lateral flow of water on or below land surface (i.e., runoff) occurs when rainfall rate exceeds soil infiltration rate, which generates a two-dimensional runoff field that is hard to measure. The runoff converges into streams and rivers, where it may exchange with groundwater and generate streamflow that can and has been monitored by stream gauges at many locations around the world's major rivers (Dai 2016). Stream gauges measure upstream basin-integrated runoff, and the gauge records have been used to calibrate model simulations (Fekete et al. 2002; Collins et al. 2024; Wade et al. 2025; Yang et al. 2025) and to quantify long-term changes in river flows (Dai et al. 2009). The runoff leaving the continents—continental runoff or discharge—is an important flux of the global water cycle (Milliman et al. 2008; Trenberth et al. 2007; Dai and Trenberth 2025) that returns the oceanic net water flux into the atmosphere back into the seas. The river outflow also discharges large amounts of minerals into the oceans (e.g., Feng et al. 2025), thereby playing a crucial role in coastal marine environments. Because continental discharge occurs primarily at the mouths of the world's large rivers, it alters local ocean salinity, density, and circulations (Coadou-Chaventon et al. 2024; Aroucha et al. 2025). In recent years, demand for freshwater has been rising together with population growth (Bogardi et al. 2013). River streamflow and continental discharge represent the renewable freshwater resource available to us. Therefore, their variations and long-term trends are important to water managers (Vörösmarty et al. 2000; Haddeland et al. 2014).

As described in Dai (2016), streamflow changes have been analyzed over many individual river basins, countries, or regions [see Dai (2016) for a long list of references]. Streamflow records show large interannual-to-decadal variations for the world's major rivers, with insignificant trends for most of them (Cluis and Laberge 2001; Lammers et al. 2001; Pekárová et al. 2003; Dai et al. 2009; Labat 2010; Dai 2016, 2021). Nevertheless, increased streamflow has been observed over areas with rising precipitation since the 1950s, such as southeastern South America (Genta et al. 1998; Pasquini and Depetris 2007), the central United States (Lins and Slack 1999; Groisman et al. 2001; Qian et al. 2007), and northern high latitudes (Peterson et al. 2002; Rawlins et al. 2006). Decreased streamflow was seen over regions with decreasing precipitation since 1950 (Dai 2021), such as in Africa,

Denotes content that is immediately available upon publication as open access.

Corresponding author: Aiguo Dai, adai@albany.edu

DOI: 10.1175/JHM-D-26-0008.1

© 2026 American Meteorological Society. This published article is licensed under the terms of the default AMS reuse license. For information regarding reuse of this content and general copyright information, consult the AMS Copyright Policy (www.ametsoc.org/PUBSReuseLicenses).

Unauthenticated | Downloaded 11/10/26 12:53 PM UTC

South and East Asia, southern Europe, and eastern Australia during recent decades (Dai et al. 2009; Dai 2016), and some river basins in Canada during the second half of the twentieth century (Zhang et al. 2001). Recent warming likely led to earlier snowmelt and peak streamflow in the western (Cayan et al. 2001) and northeastern United States (Hodgkins et al. 2003) and earlier breakup of river ice in many Canadian (Zhang et al. 2001) and Russian Arctic rivers (Smith 2000).

Global analyses of river outflow for quantifying continental freshwater discharge into the oceans are often hampered by a lack of global datasets, leading to large uncertainties in such estimates (Peel and McMahon 2006). Earlier estimates of continental discharge used interpolated data from a limited number of gauge observations (Marcinek 1964; Baumgartner and Reichel 1975; Grabs et al. 1996; Korzun 1978; L'vovich 1979; Dettinger and Diaz 2000). Recent estimates used more downstream gauge data and model-simulated runoff to complement the observations (Dai and Trenberth 2002; Dai et al. 2009; Clark et al. 2015; Dai 2016, 2021). Other estimates of continental runoff used observations together with model simulations (Döll et al. 2003; Fekete et al. 2002; Wilkinson et al. 2014) or model simulations only (Nijssen et al. 2001; McCabe and Wolock 2011; Munier et al. 2012). Recent satellite observations have also been used to extend the declining streamflow records (Elmi et al. 2024) and to estimate discharge changes (Syed et al. 2010). Recent work to combine model simulations with daily streamflow observations (Collins et al. 2024; Wade et al. 2025; Yang et al. 2025) focused on quantifying river water storages and global estimates of daily runoff and river flows since 1980.

Quantifying long-term changes in continental discharge is challenging due to a lack of data. Using data from only 50 major rivers, Probst and Tardy (1987, 1989) showed large decadal-to-multidecadal variations in discharges from individual continents and an increasing trend in South American discharge from the early twentieth century to 1980. Largely based on records from 10 rivers, Labat et al. (2004) reported an upward trend in global river discharge during the twentieth century, which has been attributed to the runoff increases resulting from either increased water use efficiency by plants under elevated carbon dioxide (CO_2) (Gedney et al. 2006) or land-use and climate changes (Piao et al. 2007). However, the result of Labat et al. (2004) was questioned by others (Legates et al. 2005; Peel and McMahon 2006; Dai et al. 2009) because of insufficient streamflow data and possible effects of nonclimatic changes such as human withdrawal of stream water (Döll et al. 2009; Biemans et al. 2011; Zhou et al. 2016). Recent comprehensive analyses (Milliman et al. 2008; Dai et al. 2009; Dai 2016, 2021) do not show significant increases since 1950 in global continental discharge but large interannual–decadal variations associated with tropical Pacific sea surface temperature (SST) variations and insignificant streamflow trends for most of the world's large rivers (Dai et al. 2009; Alkama et al. 2013). Human activities, such as withdrawal or diversion of stream water, building large dams and reservoirs, and land-use changes, may induce decadal changes and long-term declines in streamflow. Hydrological modeling (Döll et al. 2009) indicates that long-term mean global discharge into the oceans and inland seas was reduced by 2.7% due to water withdrawals and by 0.8% due to dams. This human influence is important mainly for arid-to-semiarid river basins (Milliman et al. 2008), with climate change still controlling annual flow trends for most of the world's major rivers (Dai et al. 2009).

To reliably estimate global continental discharge, we need long-term records of downstream river flow rates around all coastal lines. There are relatively few global datasets suitable for estimating continental discharge and its long-term changes. One such dataset is the Dai and Trenberth global river flow and discharge dataset (Dai and Trenberth 2002; Dai et al. 2009), which is freely available from NCAR (https://rda.ucar.edu/datasets/d551000/) but only has data up to December 2018 (Dai 2021). This dataset was created by compiling streamflow records from the downstream stations for the world's 925 largest rivers from various sources, from which yearly continental discharge since 1948 was estimated. The main goal of the dataset is to provide long-term time series estimates of continental discharge into the oceans, rather than for terrestrial hydrological research—the focus of many recent efforts to produce high-resolution runoff and streamflow data over global land using model simulations calibrated with daily streamflow observations (e.g., Collins et al. 2024; Wade et al. 2025; Yang et al. 2025). The dataset has been widely used for quantifying the global water cycle and its changes and variability (Liu et al. 2006; Clark et al. 2015; Akpoti et al. 2024; Boukthir and Abdennadher 2025) and biogeochemical cycles (Feng et al. 2025) and in ocean modeling (Coadou-Chaventon et al. 2024; Aroucha et al. 2025) and climate model evaluation (Collins et al. 2011; Lawrence et al. 2011). Here, we present a major effort to update this dataset using available streamflow records and analyze recent changes in streamflow for the world's largest rivers and in continental discharge, with updated figures resembling many of those shown previously (e.g., Dai et al. 2009; Dai 2016, 2021) with similar figure captions.

2. Streamflow data sources and methods

The Dai and Trenberth global river flow and discharge dataset (Dai and Trenberth 2002; Dai et al. 2009) contains monthly streamflow time series (for all years with data) from the farthest downstream station for the world's 925 largest rivers (selected based on their physical sizes and availability of data; see Dai and Trenberth 2002) across all continents (except Greenland and Antarctica). For estimating continental discharge, these downstream flow rates were converted into river mouth outflow rates by scaling the observed downstream flow by a mouth-to-station flow ratio based on numerically simulated flow rates (Dai and Trenberth 2002). The estimated mouth flow rates, together with contributions from the unmonitored areas (Dai and Trenberth 2002), were summed up to derive the annual discharge into the ocean through each coastal grid box, as well as yearly time series of total discharges from each continent and all continents. Thus, the Dai and Trenberth dataset contains the time series of monthly streamflow from the farthest downstream station for the world's 925 largest rivers with varying lengths, time series of annual discharge into individual and global oceans since 1949, and long-term mean two-dimensional annual freshwater

Unauthenticated | Downloaded 11/10/26 12:53 PM UTC

TABLE 1. Sources of monthly streamflow data used in this study. The symbol * denotes that these data sources were not used in previous versions of the dataset. The symbol ** denotes that of the two basin-averaged series, only the one having the stronger correlation with the observed streamflow was used to update the yearly streamflow series for the recent years.

Dataset name	Description	No. of stations used	Reference or online link
GRDC global streamflow database	Daily and monthly streamflow data from 9000+ stations over the world, but many stations only have data for a few decades during 1950–90, updated but may lag real time by several years	275	https://grdc.bafg.de/
National Water Agency of Brazil	Daily streamflow data from stations along Brazilian rivers, updated to close to real time	139	https://www.snirh.gov.br/hidroweb/serieshistoricas (in Portuguese)
USGS streamflow database	Daily and monthly streamflow or water height data from stations along most U.S. rivers, close to real time	73	https://nwis.waterdata.usgs.gov/nwis/monthly
Environment Canada streamflow database	Daily and monthly streamflow or water height data from stations along most Canadian rivers, close to real time	24	https://wateroffice.ec.gc.ca/search/statistics
Ministry of Water Resources of China*	Annual reports containing graphs and tables of monthly streamflow rates for major Chinese rivers	20	http://xxzx.mwr.gov.cn/xxgk/gbjb/
CAMELS-CL dataset*	Daily and monthly streamflow and other hydroclimatic data from 1979 to 2019 for most Chilean river basins	9	Alvarez-Garreton et al. (2018), https://camels.cr2.cl/
WHOS*	The WHOS website contains streamflow data for select locations and links to other sources	2	https://wmo.int/site/wmo-hydrohub/focus-areas/increasing-capacity/wmo-hydrological-observing-system-whos
RSEG V01*	Remote sensing–based extension of monthly discharge series up to 2022 for 3377 GRDC stations to address the recent decline in stream gauges	155	Elmi et al. (2024), https://darus.uni-stuttgart.de/dataset.xhtml?persistentId=doi:10.18419/darus-3558
GPCC full v2022	Basin-averaged monthly precipitation based on GPCC data was used to update some water-year (October–September) streamflow series when they are correlated over earlier years**	94	Schneider et al. (2022), https://opendata.dwd.de/climate_environment/GPCC/html/download_gate.html
Dai scPDSIpm	Basin-averaged monthly PDSI was used to update some water-year streamflow series when they are correlated with earlier years**	103	Dai (2021 and update), https://rda.ucar.edu/datasets/d299000/

discharge into the oceans. This dataset is freely available from NCAR (https://rda.ucar.edu/datasets/d551000/).

To update the Dai and Trenberth global river flow and discharge dataset, we gathered monthly streamflow data at the farthest downstream stations from all sources available to us (Table 1). These include new data up to December 2024 for 275 rivers around the world from the Global Runoff Data Centre (GRDC), whose database contains 460 stations used by the Dai and Trenberth dataset, 139 Brazilian rivers from the National Water Agency of Brazil, 73 U.S. rivers from the U.S. Geological Survey (USGS), 24 Canadian rivers from Environment Canada, 20 Chinese rivers from the Ministry of Water Resources of China, 9 Chilean rivers from the Catchment Attributes and Meteorology for Large-Sample Studies-Chile (CAMELS-CL) dataset, and 2 rivers (No. 8 Parana and No. 112 Pur) from the WMO Hydrological Observing System (WHOS). In general, the streamflow data from these sources looked reliable, although occasionally spurious outliers do exist in some of the time series (we did not attempt to exclude such outliers).

To address the declining number of active gauges since the 1980s in the GRDC dataset, Elmi et al. (2024) utilized satellite imagery- and altimetry-derived river width and water height observations to extend GRDC's inactive gauge series for recent years; they showed that the remote sensing–based estimates have an RMSE generally less than 30% and a correlation of 0.2–0.9 with in situ records for most stations, with better performance for large rivers. Thus, we used the remote sensing–based estimates from Elmi et al. (2024) to extend the monthly flow series for recent years. We required that the Remote Sensing–Based Extension for GRDC (RSEG) V01 monthly flow series, which includes old station data (when available) and satellite-extended flow rates for most recent years (when station data were unavailable at that time), be strongly correlated (with a correlation coefficient $r \geq 0.9$) with the updated station data (from all sources) at the collocated GRDC station. This

Unauthenticated | Downloaded 11/10/26 12:53 PM UTC

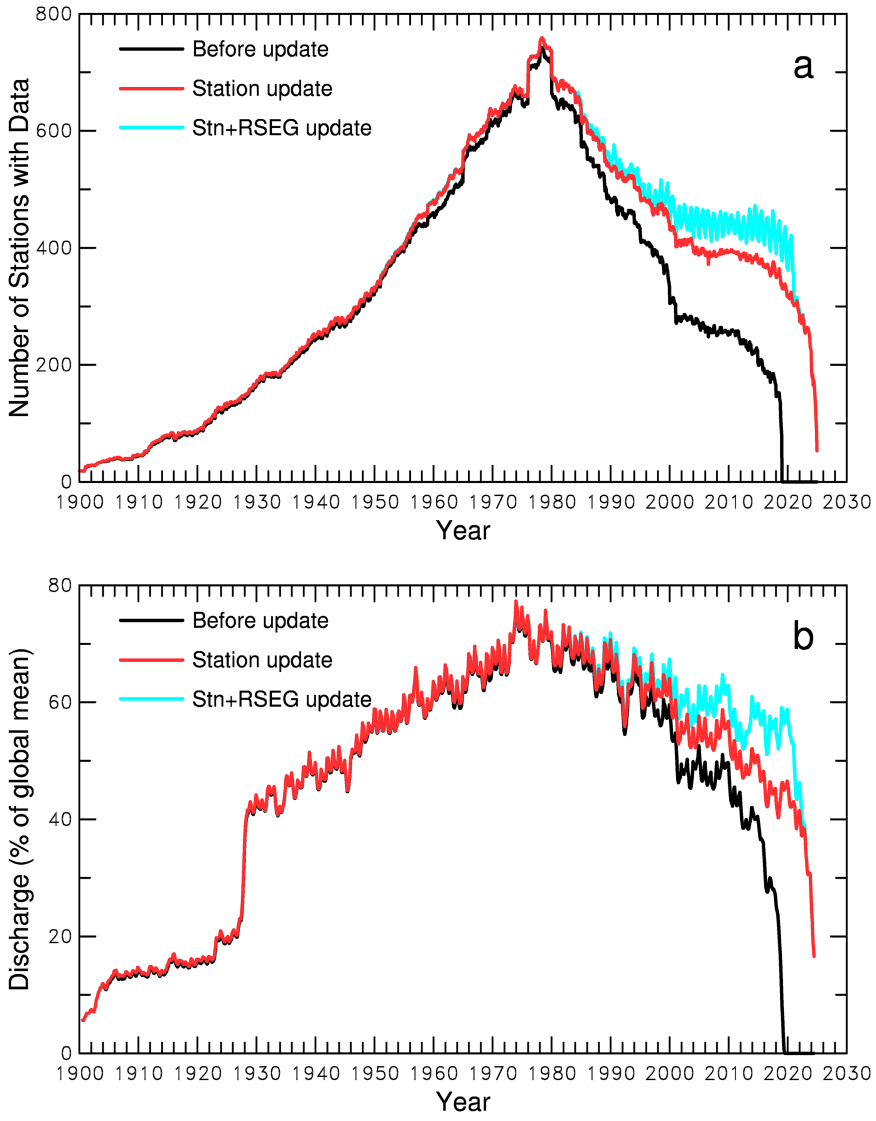


FIG. 1. (a) Monthly time series of the number of stations with data in the dataset before this update (black line), after the update using station observations (red line), and using both station data and satellite estimates of RSEG V01 (blue line). There are fewer than 200 rivers with data for 2024. (b) 13-monthly smoothed time series of the discharge (in % of the 1949–2004 mean global discharge of 1.156 Sv; Dai et al. 2009) from the stations with data. For estimating the discharge, the downstream station streamflow was adjusted to river mouth flow using the mouth-to-station flow ratio of Dai and Trenberth (2002).

resulted in updates for 155 rivers for the most recent years (up to 2022) in the GRDC database used here. The RSEG V01 data were used to infill any remaining data gaps in the updated station data series for these 155 rivers. We also examined two other satellite-based streamflow datasets, namely, the Satellite Altimetry-Based Extension of Global-Scale In Situ River Discharge Measurements (SAEM) (Saemian et al. 2024) and ESA Climate Change Initiative (CCI) (Tarpanelli et al. 2024) datasets, but were unable to find useful data for our update partly due to their short records that prevented us from comparison and validation with in situ station data.

The monthly streamflow series at a downstream station were updated with new station data for 542 rivers. The use of the RSEG data further increased the updated rivers to 697. However, the update extended the record length for only 504 rivers, while infilling data gaps in the earlier periods for 193 rivers. Figure 1a shows that the number of stations with in situ observations in the dataset increases steadily from 19 in 1900 to 759 in May 1978; thereafter, it decreases sharply to below 300 after 2022. This temporal evolution follows that of the GRDC database, which includes many upstream inland stations (Fekete et al. 2012; Dai 2016). The sharp decline in

Unauthenticated | Downloaded 11/10/26 12:53 PM UTC

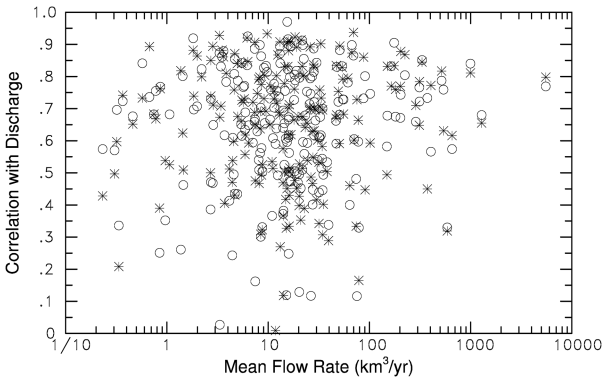


FIG. 2. Correlation coefficients between observed water-year (October–September) streamflow rates and basin-mean PDSI (stars; Dai 2011) or precipitation (circles) during 1948–2024 for the world's 200 largest rivers (based on their discharge rates) plotted as a function of the 1948–2024 mean flow rate of the corresponding river. The other smaller rivers contribute only slightly to global continental discharge (Dai and Trenberth 2002).

streamflow gauges since the 1980s is a major issue for monitoring and studying the global water cycle under a changing climate, and it can be prevented with minimum investments and increased sharing of streamflow data, as suggested previously (e.g., Fekete et al. 2012, 2015). Our assessment of the existing satellite-based streamflow datasets suggests that they are less reliable and in situ observations are still needed.

The update using the station observations increases the number of stations slightly from 1957 to 1980 and substantially since the 1980s, and the use of the RSEG V01 satellite data further increases the coverage noticeably from 1990 to 2021. Following the evolution of the station numbers, the percentage of global discharge accounted for by the stations also peaks in the 1970s (at ~75% around 1974) and then decreases steadily to less than 40% after 2022 (Fig. 1b). The jump around 1928 in Fig. 1b is due to the inclusion of the Amazon River, whose discharge accounts for ~17% of the global discharge. The update increases the discharge from the stations noticeably after 1996 using the new station data and further using the RSEG 01 data (Fig. 1b). However, even after these updates, for 2024, there are fewer than 200 stations with data and they account for less than 30% of the global discharge.

Water-year (October–September) mean flow is often significantly correlated with basin-averaged water-year precipitation or Palmer drought severity index (PDSI) (Fig. 2; Dai et al. 2009; Dai 2016, 2021), and thus, the latter two were used to extend the water-year streamflow series when it is correlated with one of them (after the above updates), which resulted in updates of water-year streamflow for 199 rivers. We required the correlation to be higher than 0.3 in order for the basin-mean PDSI or precipitation to be used to infill yearly streamflow data gaps, which were first infilled (before applying the PDSI or precipitation data) using correlated streamflow data from an upstream station when available or a land model-simulated streamflow (when highly correlated with observed streamflow and for gaps before 2005, see Dai et al. 2009). Out of the 199 rivers updated here using correlated PDSI or precipitation, only 21 had a correlation below 0.5 (but above 0.3) and most of these rivers were small–medium-sized rivers outside the top 50 by discharge volume. Thus, this infilling should improve the overall quality of the yearly streamflow data, although it contributes to the uncertainty of the estimated yearly discharge for recent years. Note that this update does not affect the station's monthly flow data.

In the end, yearly streamflow data for a total of 512 rivers were extended (up to December 2024) compared with the last update (up to December 2018) of Dai (2021). In particular, we were able to compile monthly flow data from 1998 to 2024

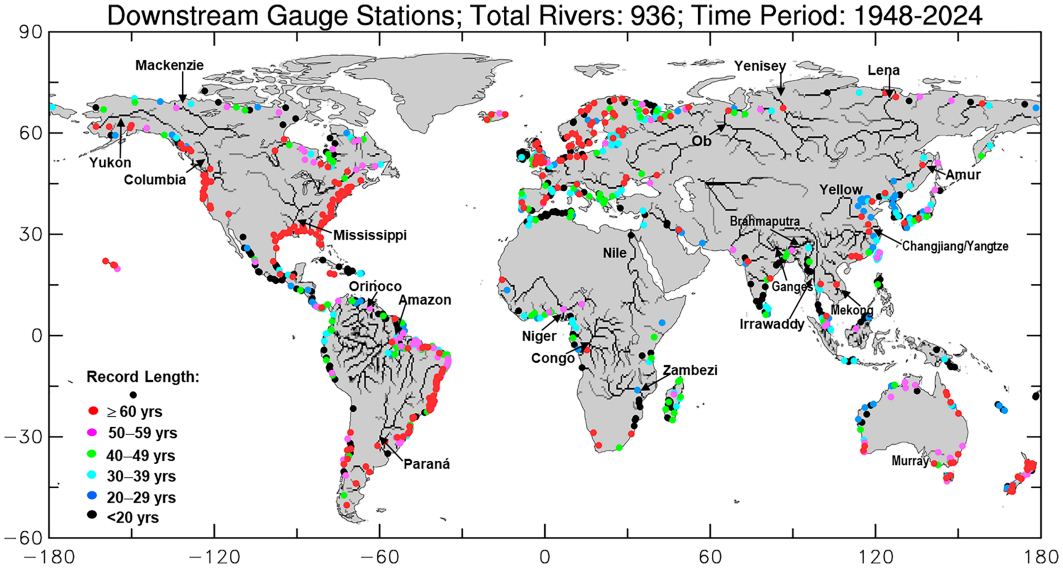


FIG. 3. Location of the farthest downstream gauge stations (dots) with different colors indicating the length of the available monthly streamflow record during 1948–2024 for the world's 936 largest rivers included in this study.

Unauthenticated | Downloaded 11/10/26 12:53 PM UTC

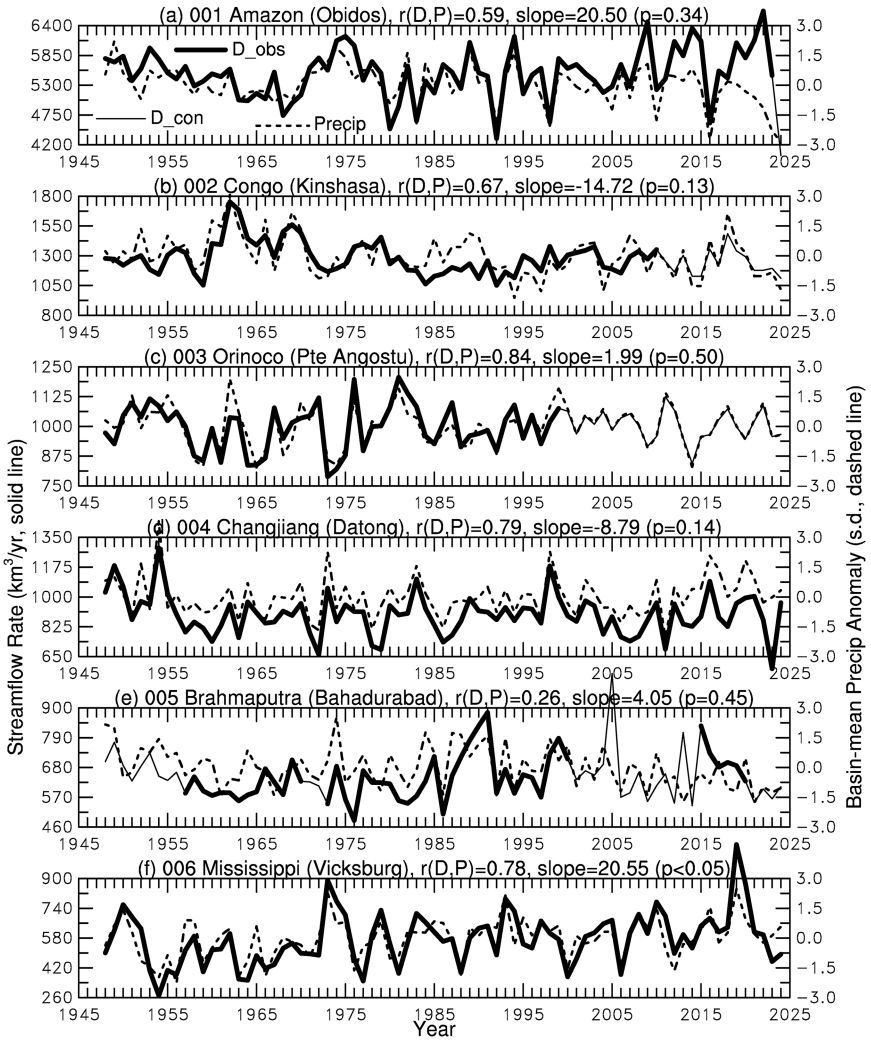


FIG. 4. (a)–(f) Time series of water-year (October–September) mean streamflow rate ($km^3\ yr^{-1}$) from 1948 (for October 1947–September 1948) to 2024 from observations (thick solid line) and estimated using either RSEG V01, basin-mean PDSI (Dai 2011), or precipitation (thin solid line) at the farthest downstream station for the world's six largest rivers, with the river name (station name) shown on top of each panel. The basin-averaged precipitation anomaly is also shown as the dashed line (right ordinate, normalized by its standard deviation) derived from rain gauge records from GPCC full v2022 (Schneider et al. 2022; for 1948–2019) extended with CRU Time Series, version 4.09 (CRU TS4.09) (Harris et al. 2020), to 2024 (after rescaling using the ratio of their monthly climatology over 1950–95). The correlation $r(D, P)$ between the thick solid and dashed lines and the slope and its p value of the linear trend of the streamflow time series (thick plus thin solid lines) are also shown. Note that for (e), the flow rates from RSEG V01 for 2005 and 2013 and station observations for 2015–20 were not well correlated with precipitation; without these recent flow rates, $r(D, P)$ increases to 0.58.

for 20 major Chinese rivers based on annual water reports released by the Ministry of Water Resources of China, which releases annual water reports at its website (Table 1) that contain monthly streamflow data at stations along major Chinese rivers either as tables or as graphs. This increases the total number of rivers from 925 to 936 in the dataset, although this change has little impact on the estimated global discharge. We also checked other online sources [e.g., those listed in Collins et al. (2024) and at the WHOS website; Table 1] but failed to find any additional new data. The inclusion of several new data sources (Table 1) in this update has improved the quality and coverage of the dataset significantly (Fig. 1).

Many major rivers in North America, Europe, and South America have near-complete streamflow records at the farthest downstream station during 1948–2024 (Fig. 3). However, available streamflow data for many large rivers in South and

Unauthenticated | Downloaded 11/10/26 12:53 PM UTC

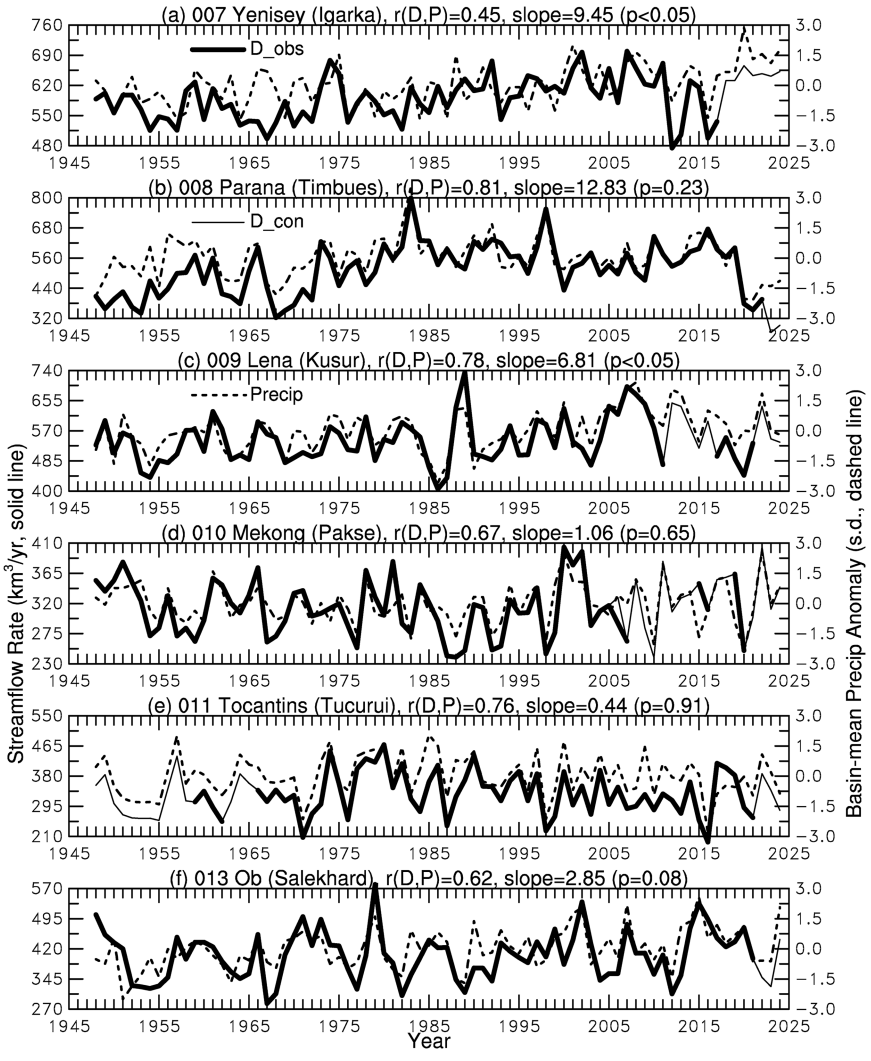


FIG. 5. As in Fig. 4, but for the world's next six largest rivers.

East Asia, Africa, and some in South America are too short (<20 years) for estimating long-term trends. Model-simulated streamflow data calibrated with in situ observations since 1980 were made available by Yang et al. (2025) after our analysis was completed. Their applicability for updating recent downstream river flow records will be explored in future updates.

While many streamflow records in our dataset start before 1948, our analysis focuses on 1948–2024. For water year 1948, it refers to October 1947–September 1948. For comparison with precipitation trends, the period 1950–2024 was used as precipitation trends since 1950 were often examined in other studies. The global discharge estimate of Dai et al. (2009), used in Fig. 7, starts from water year 1949, as model-simulated data were unavailable for 1947.

3. Streamflow measurement errors

For the U.S., Canadian, and Brazilian rivers and in many other countries, streamflow is commonly derived by converting measurements of stage heights (i.e., river water level height) into discharge rates using a locally calibrated empirical relationship between stage height and discharge (i.e., the stage-discharge rating curve). Measurement errors for stage height are typically random with small mean biases, with the random uncertainty ranging from a few percentages up to 17% depending on the measurement methods (Kiang et al. 2018). The rating curve typically is more accurate for medium flows but has large errors for high and low flow rates, leading to an overall uncertainty of discharge estimates around 3%–17% for median flows but may reach 40%–200% for high flows (Kiang et al. 2018). Streamflow measurement uncertainty for other methods typically ranges from a few percentages to 20% (McMillan et al. 2012). The USGS targets a measurement error within 10% (Fekete et al. 2012), but large errors (up to 40% or more) are reported for some measurements (Di Baldassarre and Montanari 2009; Turnipseed and Sauer 2010; Hamilton and Moore 2012; McMillan et al. 2012, 2018). The use of the acoustic Doppler current profilers (ADCPs) since the late 1990s in the

Unauthenticated | Downloaded 11/10/26 12:53 PM UTC

United States and other countries has reduced the uncertainty to less than 6% (Levin et al. 2023).

The streamflow measurement errors are typically random, so that temporal averaging (e.g., from daily flows to monthly or annual mean flows) should greatly reduce the uncertainty range. Thus, for the monthly and annual flow rates included in this dataset, the measurement uncertainty is likely to be within 10%, although outliers may exist due to recording errors. While the measurement uncertainty is important for quantitative analysis such as basin-scale water budget analysis and model evaluation, the mean biases and temporal homogeneity of the streamflow records are more important for long-term change analysis as temporal changes in the mean biases of the measurements can induce spurious long-term changes. Unlike rain gauge measurements, mean biases in streamflow gauge measurements tend to be small and their temporal changes are likely negligible, although more analyses are needed to assess the homogeneity of the streamflow records.

4. Historical changes in streamflow and runoff

Figures 4 and 5 show the time series of yearly (October–September) mean streamflow rate from 1948 (for October 1947–September 1948) to 2024 from observations (thick solid line) and estimated using basin-mean PDSI or precipitation (thin solid line) at the farthest downstream station together with observed basin-mean precipitation anomaly (dashed line) for the world's 12 largest rivers. The use of October (of the prior year) to September (of the current year) mean increases the correlation with the October–September streamflow, as snowfall of the prior winter contributes to the streamflow in the same water year for northern latitudes. This also reduces the effect of dams, whose impact is large on seasonal flows but usually small on yearly flows (Ye et al. 2003; Döll et al. 2009; Biemans et al. 2011). Interannual-to-decadal variations dominate all the streamflow series for the 12 largest rivers, with significant long-term increases since the 1950s only for the Mississippi, Yenisey, and Lena rivers. The observed yearly streamflow R and precipitation P are strongly correlated for most of the rivers, with r ranging from about 0.5 to 0.8, except for the Brahmaputra, whose flow rates after 2000 were updated using RSEG V01 and are not well correlated with P. Given the complex terrain for this river basin, it is possible that the remote sensing–based estimates may be unreliable for this basin. The high consistency between the R and P series suggests that their variations and changes are likely to be real rather than resulting from observational errors since such errors for R and P are likely uncorrelated. It also implies that climatic forcing such as P is the main driver of the observed streamflow changes for these large rivers, while direct human influences through damming and withdrawal of stream water (Biemans et al. 2011; Zhou et al. 2016) are likely small on the yearly flow, which is likely true for most of the world's major rivers (Dai et al. 2009). Nevertheless, considerable deviations between the R and P variations and changes do exist (Figs. 4 and 5), and they reflect influences on R from evapotranspiration, melting of land ice (e.g., for Yenisey, Adam and Lettenmaier 2008; Dai et al. 2009), human activities (only secondary compared with climatic forcing but could be significant for rivers in semiarid regions such as the Nile River and Indus River), and errors in the R and P data.

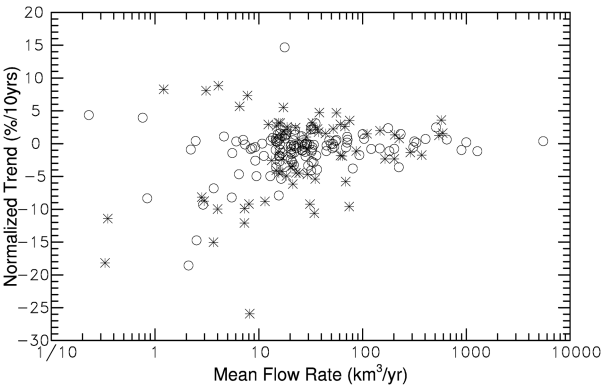


FIG. 6. Linear trends (% of the mean on the x axis per decade) of water-year (October–September) mean streamflow during 1948–2024 for the world's 200 largest rivers plotted as a function of their 1948–2024 mean flow rates. The statistically significant trends (at the 5% level) are denoted by stars (*) and insignificant ones by open circles (o). Only 71 of the 200 rivers show significant trends, with 34 being positive and 37 being negative. Smaller rivers were excluded in this plot as they do not contribute significantly to global continental discharge.

Streamflow trends over 1950–2024 are statistically insignificant for most large rivers (Fig. 6). For the top 200 rivers, only 71 (35.5%) exhibit statistically significant trends, with 34 being positive and 37 being negative. The basinwide runoff trends inferred by the downstream flow trends do, however, show coherent spatial patterns (Fig. 7a) that are broadly comparable with the observed precipitation trends during 1950–2024 (Fig. 7b), with the latter showing more spatial variations. Thus, the streamflow and inferred runoff trends likely resulted mainly from changes in precipitation rather than sampling noise. That is, these are physically meaningful trends despite the fact that they may be statistically insignificant, as noticed by Dai (2016). Figure 7 shows that during 1950–2024, precipitation and runoff increased over the central and Northeast United States, northern Europe and most of Russia, Argentina and Uruguay, and northwestern Australia but decreased over most of Africa, East and South Asia, eastern Australia, the western United States, western and eastern Canada, and parts of Brazil, similar to the trend patterns shown by Dai (2016, 2021). As pointed out previously (Dai 2016, 2021), these regional trends in both precipitation and runoff likely resulted partly from multidecadal internal climate variations, such as the interdecadal Pacific oscillation (IPO; Dai 2013; Dong and Dai 2015), and recent global warming (Zhang et al. 2007; Gu and Adler 2023; Dai and Trenberth 2025).

The streamflow-inferred runoff trends and observed precipitation trends differ over some regions (Fig. 7). For example, the precipitation trend over Brazil exhibits considerable spatial variations, while the inferred basin-mean runoff trends are more coherent with increases in the west and decreases in the east (Fig. 7). The P and R trends over central Europe and most of

Unauthenticated | Downloaded 11/10/26 12:53 PM UTC

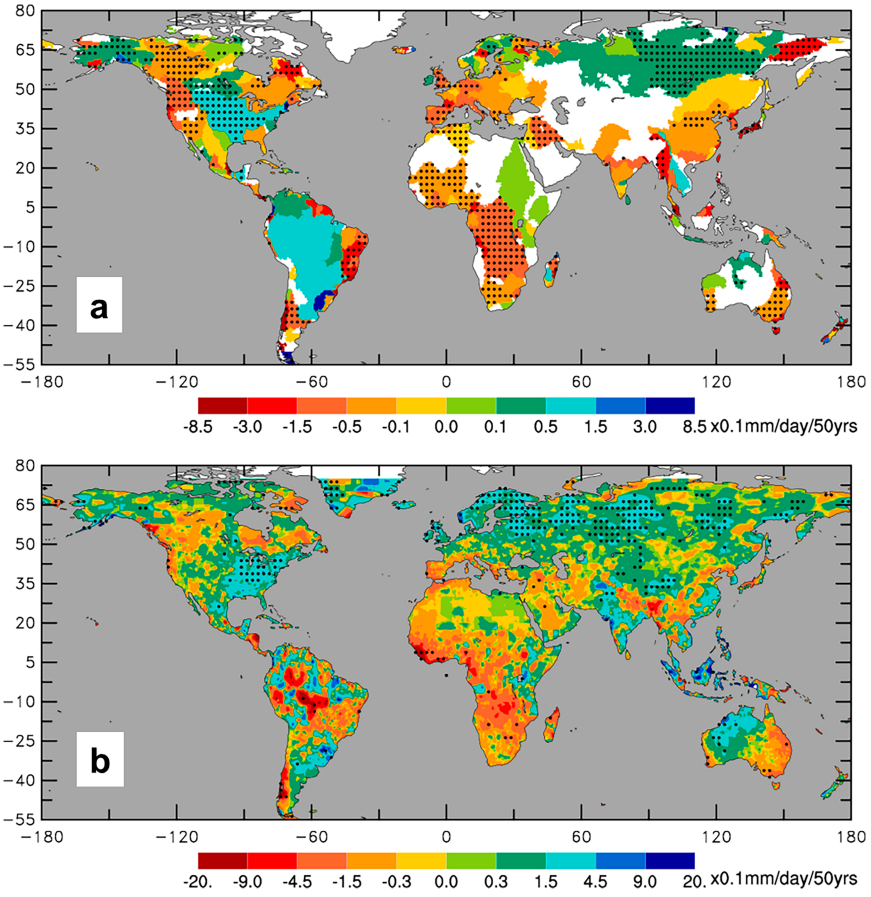


FIG. 7. (a) Long-term (1950–2024) trends [0.1 mm day^{-1} (50 yr)$^{-1}$] of October–September (i.e., 1950 is for October 1949–September 1950) mean runoff inferred from observed downstream river flow rates. Blank areas do not have runoff into the oceans or enough observations. (b) As in (a), but for trends in annual (January–December) precipitation derived from rain gauge records by GPCC full v2022 (Schneider et al. 2022; for 1948–2019) extended with CRU TS4.09 (Harris et al. 2020) to 2024 (after rescaling using the ratio of their monthly climatology over 1950–95). Precipitation trends from CRU TS4.09 are very similar.

India also appear to have opposite signs. Some of these inconsistencies may be related to spatial mismatch of these two fields as the inferred runoff trend reflects the basin mean rather than the local precipitation trend.

The global (excluding Greenland and Antarctica) continental discharge using estimates by Dai et al. (2009) for 1949–2004 and by this study for 2005–23 (station coverage is too low for 2024), together with global (60°S–75°N) land mean precipitation, is shown in Fig. 8. We used the updated streamflow data for the 512 largest rivers to derive a yearly series of discharges from these rivers, which account for about 70% of the global discharge. This estimated discharge is strongly correlated (r = 0.90) with the global discharge from Dai et al. (2009) over 1949–2004 (thick solid line in Fig. 8); thus, we used it to estimate the global discharge for 2005–23 (thin solid line in Fig. 8) through linear regression over 1949–2004 with the thick solid line in Fig. 8, following Dai (2016, 2021). This regression-based estimate of global discharge for 2005–23 is likely less reliable than the direct estimate for 1949–2004, especially for the last few years when many rivers do not have data (Fig. 1). Figure 8 also shows the October–September mean precipitation anomaly averaged over global land (dashed line). Global continental discharge shows large interannual variations (e.g., a sharp drop in 1992 following the Pinatubo volcanic eruption in June 1991), with a weak decreasing trend from 1949 to 1992 [slope = −0.096 Sv (100 yr)$^{-1}$, p value = 0.01; 1 Sv ≡ 10^6 m^3 s^{-1}] and some recovery thereafter [slope = 0.158 Sv (100 yr)$^{-1}$, p value = 0.02] from 1992 to 2022. We noticed the relatively low discharge during 2005–15 compared to Dai (2021), likely due to the inclusion of more updated stream gauge data in this analysis. Land precipitation exhibits similar interannual-to-decadal variations and correlates with the discharge (r = 0.58; Fig. 8), suggesting that land precipitation is a major driver of variations and changes in continental discharge.

As noticed by previous studies (e.g., Trenberth and Dai 2007; Dai et al. 2009; Dai 2016, 2021), Pacific tropical SSTs have a major influence on both land precipitation and

Unauthenticated | Downloaded 11/10/26 12:53 PM UTC

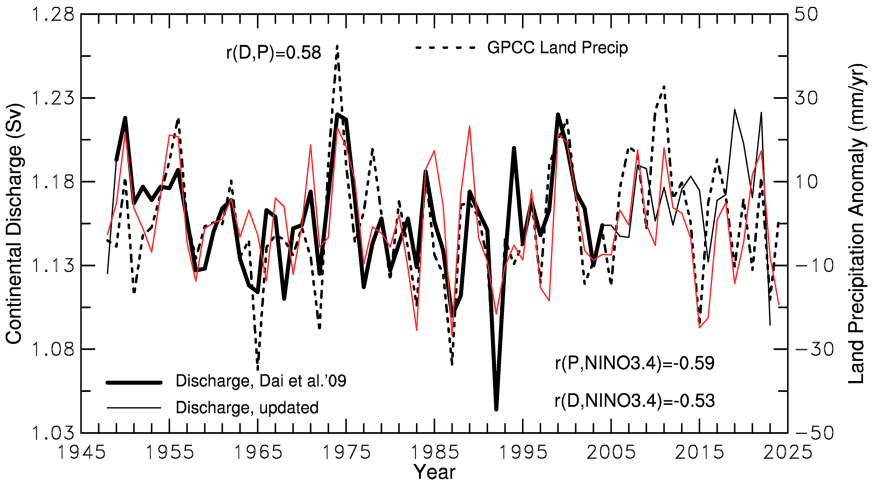


FIG. 8. Time series of October–September mean total continental discharge (Sv or 1×10^6 m^3 s^{-1}, excluding that from Greenland and Antarctica) for 1949–2004 (thick solid line) from Dai et al. (2009) and for 2005–23 (thin solid line) estimated based on updated streamflow data for the world's 512 largest rivers and a linear regression with the thick solid line. The dashed line is the October–September mean precipitation averaged over global (60°S–75°N) land areas derived from rain gauge records by GPCC full v2022 (Schneider et al. 2022; for 1948–2019) extended with CRU TS4.09 (Harris et al. 2020) to 2024 (after rescaling using the ratio of their monthly climatology over 1950–95). Also shown (red line) is the Niño-3.4 (170°–120°W, 5°S–5°N) SST index plotted positive downward. The correlations among the discharge D (including the thin solid line), land precipitation P, and Niño-3.4 SST are shown. The trend slope is -0.096 Sv (100 yr)$^{-1}$ (p value = 0.01) for 1949–92 and 0.158 Sv (100 yr)$^{-1}$ (p value = 0.02) for 1992–2022. The large drop in discharge for 2023 resulted from the estimated discharge for Amazon, Parana, and other rivers for 2023 that may be unreliable.

continental discharge, which is reflected by the significant correlation with the Niño-3.4 SST anomalies ($r = -0.59$ for precipitation and -0.53 for discharge during 1949–2023) (Fig. 8). During El Niño years, precipitation is usually below normal over many land areas in South Asia, Australia, southern and West Africa, central America, and northern South America, while it is above normal only in southern South America, the southern and central United States, and a few other land areas (Dai and Wigley 2000; Dai 2013), which leads to below-normal precipitation and runoff averaged over global land during El Niño years and the opposite (i.e., above-normal precipitation and runoff) during cold La Niña events. Dai et al. (2009) showed significant correlations (from $r = -0.50$ to -0.61) between the Niño-3.4 SST index and the discharge into the Pacific, Indian, and Atlantic Oceans. Therefore, El Niño–Southern Oscillation (ENSO) is a major source of interannual variations in land precipitation and continental discharge, as noticed previously (Dai et al. 2009; Dai 2016, 2021). Furthermore, in addition to the ENSO-induced large multiyear variations, the decadal–multidecadal variations in the ENSO SST index (i.e., the IPO; Dai 2013) are also correlated with the decadal–multidecadal changes in land precipitation and continental discharge (Fig. 8; Dong and Dai 2015). Thus, Pacific decadal variability is also an important source of the decadal variations in land precipitation and continental discharge, with below (above)-normal land precipitation and discharge during IPO's warm (cold) phase.

5. Summary

Variations and long-term changes in river streamflow and continental runoff are of great concern as they represent the renewable freshwater resource available to human society and other inhabitants on land. Streamflow in most of the world's major rivers has been monitored by stream gauges for decades, but recent streamflow data for many rivers in Asia and Africa are publicly unavailable and this hampers scientific research. More efforts are needed to collect and compile streamflow data (Fekete et al. 2012).

Here, we made a major effort to update the Dai and Trenberth streamflow and discharge dataset using available monthly streamflow data (up to December 2024) for the world's 697 largest rivers obtained from various sources (Table 1), which increases the record length for 512 rivers. The updated dataset now includes 936 rivers across all continents and islands except Greenland and Antarctica. The update increases the number of stations with data slightly for 1957–80 and substantially for 1980–2024 using both new station data and RSEG V01 satellite estimates. Nevertheless, the number of stations with data peaked at 759 around 1978 and then declined sharply to below 300 after 2022. Random measurement errors for streamflow range from less than 6% for modern acoustic Doppler current profilers used since the late 1990s to within 10% for conventional USGS measurements and up to 20%–40% for other measurements. However, such errors should be much lower for time-averaged monthly or yearly mean flow rates, although

Unauthenticated | Downloaded 11/10/26 12:53 PM UTC

timing-varying mean biases, albeit small, could affect the trends in streamflow records.

The updated time series of annual flow rates are correlated with basin-mean precipitation, indicating that the variations and changes in both streamflow and precipitation records are likely real. Long-term (1948–2024) trends in annual streamflow are statistically insignificant for most of the rivers, with only 71 (35.5%) of the top 200 rivers showing significant trends with 34 being positive and 37 being negative. Global continental discharge is dominated by large interannual variations together with considerable decadal changes; it shows a weak downward trend from 1949 to 1993; thereafter, it recovered to levels slightly above those of the 1950s–1980s. Land precipitation is the key driver of the discharge variations and changes, and the two are correlated on interannual-to-decadal time scales. ENSO is a major source of interannual variations in land precipitation and continental discharge, while IPO has a significant influence on their decadal changes during 1949–2024, with below (above) normal land precipitation and discharge during its warm (cold) phases, similar to ENSO's influence.

While recent streamflow trends are statistically insignificant for most rivers, their inferred runoff trends show coherent spatial patterns that are broadly comparable with observed precipitation trends during 1950–2024. These trends show that during 1950–2024, annual precipitation and runoff increased over the central and Northeast United States, northern Europe and most of Russia, Argentina and Uruguay, and northwestern Australia but decreased over most of Africa, East and South Asia, eastern Australia, the western United States, western and eastern Canada, and parts of Brazil. Both internal climate variability (especially IPO) and externally forced changes likely contributed to these regional trends in precipitation and runoff.

Acknowledgments. We thank the Global Runoff Data Centre (GRDC), 56068 Koblenz, Germany, for making their streamflow data available online. Dai acknowledges the funding support from the National Science Foundation (Grants AGS-2015780 and 2528650). A. Dai did most of the data analysis and wrote the draft manuscript; Hu, Guo, Liu, Liang, and Wang helped gather and compile most of the streamflow data; Duan and M. Dai helped organize the research team; and Hu, Guo, and M. Dai also helped improve the manuscript.

Data availability statement. The updated streamflow and discharge data are available from Zenodo under DOI: 10.5281/zenodo.17379716 (Dai et al. 2025). It will also be made freely available from NCAR at https://rda.ucar.edu/datasets/d551000/.

REFERENCES

Adam, J. C., and D. P. Lettenmaier, 2008: Application of new precipitation and reconstructed streamflow products to streamflow trend attribution in northern Eurasia. *J. Climate*, **21**, 1807–1828, https://doi.org/10.1175/2007JCLI1535.1.

Akpoti, K., K. Mekonnen, M. Leh, A. Owusu, M. Dembélé, P. Tinonetsana, A. Seid, and N. M. Velpuri, 2024: State of continental discharge estimation and modelling: Challenges and opportunities for Africa. *Hydrol. Sci. J.*, **69**, 2124–2152, https://doi.org/10.1080/02626667.2024.2402938.

Alkama, R., L. Marchand, A. Ribes, and B. Decharme, 2013: Detection of global runoff changes: Results from observations and CMIP5 experiments. *Hydrol. Earth Syst. Sci.*, **17**, 2967–2979, https://doi.org/10.5194/hess-17-2967-2013.

Alvarez-Garreton, C., and Coauthors, 2018: The CAMELS-CL dataset: Catchment attributes and meteorology for large sample studies—Chile dataset. *Hydrol. Earth Syst. Sci.*, **22**, 5817–5846, https://doi.org/10.5194/hess-22-5817-2018.

Aroucha, L. C., J. F. Lübbecke, P. Brandt, F. U. Schwarzkopf, and A. Biastoch, 2025: River discharge impacts coastal southeastern tropical Atlantic sea surface temperature and circulation: A model-based analysis. *Ocean Sci.*, **21**, 661–678, https://doi.org/10.5194/os-21-661-2025.

Baumgartner, A., and E. Reichel, 1975: *The World Water Balance; Mean Annual Global, Continental and Maritime Precipitation, Evaporation and Run-off.* Elsevier, 179 pp.

Biemans, H., I. Haddeland, P. Kabat, F. Ludwig, R. W. A. Hutjes, J. Heinke, W. von Bloh, and D. Gerten, 2011: Impact of reservoirs on river discharge and irrigation water supply during the 20th century. *Water Resour. Res.*, **47**, W03509, https://doi.org/10.1029/2009WR008929.

Bogardi, J. J., B. M. Fekete, and C. J. Vörösmarty, 2013: Planetary boundaries revisited: A view through the 'water lens'. *Curr. Opin. Environ. Sustainability*, **5**, 581–589, https://doi.org/10.1016/j.cosust.2013.10.006.

Boukthir, M., and J. Abdennadher, 2025: Climatological seasonal cycle of river discharge into the oceans: Contributions from major rivers and implications for ocean modeling. *Hydrology*, **12**, 147, https://doi.org/10.3390/hydrology12060147.

Cayan, D. R., S. A. Kammerdiener, M. D. Dettinger, J. M. Caprio, and D. H. Peterson, 2001: Changes in the onset of spring in the western United States. *Bull. Amer. Meteor. Soc.*, **82**, 399–416, https://doi.org/10.1175/1520-0477(2001)082<0399:CITOOS>2.3.CO;2.

Clark, E. A., J. Sheffield, M. T. H. van Vliet, B. Nijssen, and D. P. Lettenmaier, 2015: Continental runoff into the oceans (1950–2008). *J. Hydrometeor.*, **16**, 1502–1520, https://doi.org/10.1175/JHM-D-14-0183.1.

Cluis, D., and C. Laberge, 2001: Climate change and trend detection in selected rivers within the Asia-Pacific region. *Water Int.*, **26**, 411–424, https://doi.org/10.1080/02508060108686933.

Coadou-Chaventon, S., S. Speich, D. Zhang, C. B. Rocha, and S. Swart, 2024: Oceanic fronts driven by the Amazon freshwater plume and their thermohaline compensation at the submesoscale. *J. Geophys. Res. Oceans*, **129**, e2024JC021326, https://doi.org/10.1029/2024JC021326.

Collins, E. L., and Coauthors, 2024: Global patterns in river water storage dependent on residence time. *Nat. Geosci.*, **17**, 433–439, https://doi.org/10.1038/s41561-024-01421-5.

Collins, W. J., and Coauthors, 2011: Development and evaluation of an Earth-system model—HadGEM2. *Geosci. Model Dev.*, **4**, 1051–1075, https://doi.org/10.5194/gmd-4-1051-2011.

Dai, A., 2011: Characteristics and trends in various forms of the Palmer drought severity index during 1900–2008. *J. Geophys. Res.*, **116**, D12115, https://doi.org/10.1029/2010JD015541.

——, 2013: The influence of the inter-decadal Pacific oscillation on US precipitation during 1923–2010. *Climate Dyn.*, **41**, 633–646, https://doi.org/10.1007/s00382-012-1446-5.

——, 2016: Historical and future changes in streamflow and continental runoff: A review. *Terrestrial Water Cycle and Climate Change: Natural and Human-Induced Impacts, Geophys.*

Unauthenticated | Downloaded 11/10/26 12:53 PM UTC

Monogr., Vol. **221**, Amer. Geophys. Union, 17–37, https://doi.org/10.1002/9781118971772.ch2.

——, 2021: Hydroclimatic trends during 1950–2018 over global land. *Climate Dyn.*, **56**, 4027–4049, https://doi.org/10.1007/s00382-021-05684-1.

——, and T. M. L. Wigley, 2000: Global patterns of ENSO-induced precipitation. *Geophys. Res. Lett.*, **27**, 1283–1286, https://doi.org/10.1029/1999GL011140.

——, and K. E. Trenberth, 2002: Estimates of freshwater discharge from continents: Latitudinal and seasonal variations. *J. Hydrometeor.*, **3**, 660–687, https://doi.org/10.1175/1525-7541(2002)003<0660:EOFDFC>2.0.CO;2.

——, and ——, 2025: The water cycle. *Reference Module in Encyclopedia of Climate System Science*. Elsevier, 1–21, https://doi.org/10.1016/B978-0-443-15748-6.00034-4.

——, T. T. Qian, K. E. Trenberth, and J. D. Milliman, 2009: Changes in continental freshwater discharge from 1948 to 2004. *J. Climate*, **22**, 2773–2792, https://doi.org/10.1175/2008JCLI2592.1.

——, J. Hu, A. Duan, X. Guo, M. Liu, R. Liang, G. Wang, and M. Dai, 2025: The Dai downstream river flow and continental discharge dataset. Zenodo, accessed 20 November 2025, https://doi.org/10.5281/zenodo.17379716.

Dettinger, M. D., and H. F. Diaz, 2000: Global characteristics of stream flow seasonality and variability. *J. Hydrometeor.*, **1**, 289–310, https://doi.org/10.1175/1525-7541(2000)001<0289:GCOSFS>2.0.CO;2.

Di Baldassarre, G., and A. Montanari, 2009: Uncertainty in river discharge observations: A quantitative analysis. *Hydrol. Earth Syst. Sci.*, **13**, 913–921, https://doi.org/10.5194/hess-13-913-2009.

Döll, P., F. Kaspar, and B. Lehner, 2003: A global hydrological model for deriving water availability indicators: Model tuning and validation. *J. Hydrol.*, **270**, 105–134, https://doi.org/10.1016/S0022-1694(02)00283-4.

——, K. Fiedler, and J. Zhang, 2009: Global-scale analysis of river flow alterations due to water withdrawals and reservoirs. *Hydrol. Earth Syst. Sci.*, **13**, 2413–2432, https://doi.org/10.5194/hess-13-2413-2009.

Dong, B., and A. Dai, 2015: The influence of the interdecadal Pacific oscillation on temperature and precipitation over the globe. *Climate Dyn.*, **45**, 2667–2681, https://doi.org/10.1007/s00382-015-2500-x.

Elmi, O., M. J. Tourian, P. Saemian, and N. Sneeuw, 2024: Remote sensing-based extension of GRDC discharge time series—A monthly product with uncertainty estimates. *Sci. Data*, **11**, 240, https://doi.org/10.1038/s41597-024-03078-6.

Fekete, B. M., C. J. Vörösmarty, and W. Grabs, 2002: High-resolution fields of global runoff combining observed river discharge and simulated water balances. *Global Biogeochem. Cycles*, **16**, 1042, https://doi.org/10.1029/1999GB001254.

——, U. Looser, A. Pietroniro, and R. D. Robarts, 2012: Rationale for monitoring discharge on the ground. *J. Hydrometeor.*, **13**, 1977–1986, https://doi.org/10.1175/JHM-D-11-0126.1.

——, R. D. Robarts, M. Kumagai, H.-P. Nachtnebel, E. Odada, and A. V. Zhuliov, 2015: Time for in situ renaissance. *Science*, **349**, 685–686, https://doi.org/10.1126/science.aac7358.

Feng, D., Z. Tan, S. Pinel, D. Xu, J. H. F. Amaral, A. C. Fassoni-Andrade, M.-P. Bonnet, and G. Bisht, 2025: Drivers and impacts of sediment deposition in Amazonian floodplains. *Nat. Commun.*, **16**, 3148, https://doi.org/10.1038/s41467-025-57495-1.

Gedney, N., P. M. Cox, R. A. Betts, O. Boucher, C. Huntingford, and P. A. Stott, 2006: Detection of a direct carbon dioxide effect in continental river runoff records. *Nature*, **439**, 835–838, https://doi.org/10.1038/nature04504.

Genta, J. L., G. Perez-Iribarren, and C. R. Mechoso, 1998: A recent increasing trend in the streamflow of rivers in southeastern South America. *J. Climate*, **11**, 2858–2862, https://doi.org/10.1175/1520-0442(1998)011<2858:ARITIT>2.0.CO;2.

Grabs, W. E., T. de Couet, and J. Pauler, 1996: Freshwater fluxes from continents into the world oceans based on data of the global runoff data base. GRDC Rep. 10, 49 pp. + annex 179 pp., 231 pp., https://doi.bafg.de/BfG/1996/GRDC_Report_10.pdf.

Groisman, P. Ya, R. W. Knight, and T. R. Karl, 2001: Heavy precipitation and high streamflow in the contiguous United States: Trends in the twentieth century. *Bull. Amer. Meteor. Soc.*, **82**, 219–246, https://doi.org/10.1175/1520-0477(2001)082<0219:HPAHSI>2.3.CO;2.

Gu, G., and R. Adler, 2023: Observed variability and trends in global precipitation during 1979–2020. *Climate Dyn.*, **61**, 131–150, https://doi.org/10.1007/s00382-022-06567-9.

Haddeland, I., and Coauthors, 2014: Global water resources affected by human interventions and climate change. *Proc. Natl Acad. Sci. USA*, **111**, 3251–3256, https://doi.org/10.1073/pnas.1222475110.

Hamilton, A. S., and R. D. Moore, 2012: Quantifying uncertainty in streamflow records. *Can. Water Resour. J.*, **37**, 3–21, https://doi.org/10.4296/cwrj3701865.

Harris, I., T. J. Osborn, P. Jones, and D. Lister, 2020: Version 4 of the CRU TS monthly high-resolution gridded multivariate climate dataset. *Sci. Data*, **7**, 109, https://doi.org/10.1038/s41597-020-0453-3.

Hodgkins, G. A., R. W. Dudley, and T. G. Huntington, 2003: Changes in the timing of high river flows in New England over the 20th century. *J. Hydrol.*, **278**, 244–252, https://doi.org/10.1016/S0022-1694(03)00155-0.

Kiang, J. E., and Coauthors, 2018: A comparison of methods for streamflow uncertainty estimation. *Water Resour. Res.*, **54**, 7149–7176, https://doi.org/10.1029/2018WR022708.

Korzun, V. I., 1978: *World Water Balance and Water Resources of the Earth (English Translation)*. UNESCO, 663 pp.

Labat, D., 2010: Cross wavelet analyses of annual continental freshwater discharge and selected climate indices. *J. Hydrol.*, **385**, 269–278, https://doi.org/10.1016/j.jhydrol.2010.02.029.

——, Y. Goddéris, J. L. Probst, and J. L. Guyot, 2004: Evidence for global runoff increase related to climate warming. *Adv. Water Resour.*, **27**, 631–642, https://doi.org/10.1016/j.advwatres.2004.02.020.

Lammers, R. B., A. I. Shiklomanov, C. J. Vorosmarty, B. M. Fekete, and B. J. Peterson, 2001: Assessment of contemporary Arctic river runoff based on observational discharge records. *J. Geophys. Res.*, **106**, 3321–3334, https://doi.org/10.1029/2000JD900444.

Lawrence, D. M., and Coauthors, 2011: Parameterization improvements and functional and structural advances in version 4 of the Community Land Model. *J. Adv. Model. Earth Syst.*, **3**, M03001, https://doi.org/10.1029/2011MS00045.

Legates, D. R., H. F. Lins, and G. J. McCabe, 2005: Comments on "Evidence for global runoff increase related to climate warming" by Labat et al. *Adv. Water Resour.*, **28**, 1310–1315, https://doi.org/10.1016/j.advwatres.2005.04.006.

Levin, S. B., and Coauthors, 2023: Uncertainties in measuring and estimating water-budget components: Current state of the science. *Wiley Interdiscip. Rev.: Water*, **10**, e1646, https://doi.org/10.1002/wat2.1646.

Unauthenticated | Downloaded 11/10/26 12:53 PM UTC

Lins, H. F., and J. R. Slack, 1999: Streamflow trends in the United States. *Geophys. Res. Lett.*, **26**, 227–230, https://doi.org/10.1029/1998GL900291.

Liu, W. T., X. Xie, W. Tang, and V. Zlotnicki, 2006: Spacebased observations of oceanic influence on the annual variation of South American water balance. *Geophys. Res. Lett.*, **33**, L08710, https://doi.org/10.1029/2006GL025683.

L'vovich, M. I., 1979: *World Water Resources and their Future.* Amer. Geophys. Union, 415 pp.

Marcinek, J., 1964: The river discharge from land surface over the globe and its distribution in 5° zones (in German). Bulletin of the Institute of Water Management Tech. Rep. 21, 204 pp.

McCabe, G. J., and D. M. Wolock, 2011: Century-scale variability in global annual runoff examined using a water balance model. *Int. J. Climatol.*, **31**, 1739–1748, https://doi.org/10.1002/joc.2198.

McMillan, H. K., T. Krueger, and J. Freer, 2012: Benchmarking observational uncertainties for hydrology: Rainfall, river discharge and water quality. *Hydrol. Processes*, **26**, 4078–4111, https://doi.org/10.1002/hyp.9384.

——, I. K. Westerberg, and T. Krueger, 2018: Hydrological data uncertainty and its implications. *Wiley Interdiscip. Rev.: Water*, **5**, e1319, https://doi.org/10.1002/wat2.1319.

Milliman, J. D., K. L. Farnsworth, P. D. Jones, K. H. Xu, and L. C. Smith, 2008: Climatic and anthropogenic factors affecting river discharge to the global ocean, 1951–2000. *Global Planet. Change*, **62**, 187–194, https://doi.org/10.1016/j.gloplacha.2008.03.001.

Munier, S., H. Palanisamy, P. Maisongrande, A. Cazenave, and E. F. Wood, 2012: Global runoff anomalies over 1993–2009 estimated from coupled land–ocean–atmosphere water budgets and its relation with climate variability. *Hydrol. Earth Syst. Sci.*, **16**, 3647–3658, https://doi.org/10.5194/hess-16-3647-2012.

Nijssen, B., G. M. O'Donnell, D. P. Lettenmaier, D. Lohmann, and E. F. Wood, 2001: Predicting the discharge of global rivers. *J. Climate*, **14**, 3307–3323, https://doi.org/10.1175/1520-0442(2001)014<3307:PTDOGR>2.0.CO;2.

Pasquini, A. I., and P. J. Depetris, 2007: Discharge trends and flow dynamics of South American rivers draining the southern Atlantic seaboard: An overview. *J. Hydrol.*, **333**, 385–399, https://doi.org/10.1016/j.jhydrol.2006.09.005.

Peel, M. C., and T. A. McMahon, 2006: Continental runoff: A quality-controlled global runoff data set. *Nature*, **444**, E14, https://doi.org/10.1038/nature05480.

Pekárová, P., P. Miklánek, and J. Pekár, 2003: Spatial and temporal runoff oscillation analysis of the main rivers of the world during the 19th–20th centuries. *J. Hydrol.*, **274**, 62–79, https://doi.org/10.1016/S0022-1694(02)00397-9.

Peterson, B. J., R. M. Holmes, J. W. McClelland, C. J. Vörösmarty, R. B. Lammers, A. I. Shiklomanov, I. A. Shiklomanov, and S. Rahmstorf, 2002: Increasing river discharge to the Arctic Ocean. *Science*, **298**, 2171–2173, https://doi.org/10.1126/science.1077445.

Piao, S., P. Friedlingstein, P. Ciais, N. de Noblet-Ducouvré, D. Labat, and S. Zaehle, 2007: Changes in climate and land use have a larger direct impact than rising CO_2 on global river runoff trends. *Proc. Natl. Acad. Sci. USA*, **104**, 15 242–15 247, https://doi.org/10.1073/pnas.0707213104.

Probst, J. L., and Y. Tardy, 1987: Long range streamflow and world continental runoff fluctuations since the beginning of this century. *J. Hydrol.*, **94**, 289–311, https://doi.org/10.1016/0022-1694(87)90057-6.

——, and ——, 1989: Global runoff fluctuations during the last 80 years in relation to world temperature change. *Amer. J. Sci.*, **289**, 267–285, https://doi.org/10.2475/ajs.289.3.267.

Qian, T., A. Dai, and K. E. Trenberth, 2007: Hydroclimatic trends in the Mississippi River basin from 1948 to 2004. *J. Climate*, **20**, 4599–4614, https://doi.org/10.1175/JCLI4262.1.

Rawlins, M. A., C. J. Willmott, A. Shiklomanov, E. Linder, S. Frolking, R. B. Lammers, and C. J. Vörösmarty, 2006: Evaluation of trends in derived snowfall and rainfall across Eurasia and linkages with discharge to the Arctic Ocean. *Geophys. Res. Lett.*, **33**, L07403, https://doi.org/10.1029/2005GL025231.

Saemian, P., O. Elmi, M. Stroud, R. Riggs, B. M. Kitambo, F. Papa, G. H. Allen, and M. J. Tourian, 2024: Satellite Altimetry-based Extension of global-scale in situ river discharge Measurements (SAEM), DaRUS V2. DaRUS, accessed 30 April 2026, https://doi.org/10.18419/DARUS-4475.

Schneider, U., S. Hänsel, P. Finger, E. Rustemeier, and M. Ziese, 2022: GPCC full data monthly product version 2022 at 0.5°: Monthly land-surface precipitation from rain-gauges built on GTS-based and historical data. GPCC, accessed 15 April 2025, https://doi.org/10.5676/DWD_GPCC/FD_M_V2022_050.

Smith, L. C., 2000: Trends in Russian Arctic river-ice formation and breakup, 1917 to 1994. *Phys. Geogr.*, **21**, 46–56, https://doi.org/10.1080/02723646.2000.10642698.

Syed, T. H., J. S. Famiglietti, D. P. Chambers, J. K. Willis, and K. Hilburn, 2010: Satellite-based global-ocean mass balance estimates of interannual variability and emerging trends in continental freshwater discharge. *Proc. Natl. Acad. Sci. USA*, **107**, 17 916–17 921, https://doi.org/10.1073/pnas.1003292107.

Tarpanelli, A., P. Filippucci, and D. P. Sahoo, 2024: ESA River Discharge climate change initiative (RD_cci): Combined river discharge product, v1.0. NERC EDS Centre for Environmental Data Analysis, accessed 15 March 2026, https://doi.org/10.5285/d32244e674dd438ca4d321560daad755.

Trenberth, K. E., and A. Dai, 2007: Effects of Mount Pinatubo volcanic eruption on the hydrological cycle as an analog of geoengineering. *Geophys. Res. Lett.*, **34**, L15702, https://doi.org/10.1029/2007GL030524.

——, L. Smith, T. Qian, A. Dai, and J. Fasullo, 2007: Estimates of the global water budget and its annual cycle using observational and model data. *J. Hydrometeor.*, **8**, 758–769, https://doi.org/10.1175/JHM600.1.

Turnipseed, D. P., and V. B. Sauer, 2010: Discharge measurements at gaging stations. USGS Publications Warehouse Techniques and Methods Rep. 3-A8, 87 pp., https://doi.org/10.3133/tm3A8.

Vörösmarty, C. J., P. Green, J. Salisbury, and R. B. Lammers, 2000: Global water resources: Vulnerability from climate change and population growth. *Science*, **289**, 284–288, https://doi.org/10.1126/science.289.5477.284.

Wade, J., and Coauthors, 2025: Intrinsic spatial scales of river stores and fluxes and their relative contributions to the global water cycle. *Geophys. Res. Lett.*, **52**, e2024GL113052, https://doi.org/10.1029/2024GL113052.

Wilkinson, K., M. von Zabern, and J. Scherzer, 2014: Global freshwater fluxes into the world oceans. GRDC Tech. Rep. 44, 23 pp., https://doi.bafg.de/BfG/2014/GRDC_Report_44.pdf.

Yang, Y., and Coauthors, 2025: Global daily discharge estimation based on grid long short-term memory (LSTM) model and river routing. *Water Resour. Res.*, **61**, e2024WR039764, https://doi.org/10.1029/2024WR039764.

Ye, B. S., D. Q. Yang, and D. L. Kane, 2003: Changes in Lena River streamflow hydrology: Human impacts versus natural

Unauthenticated | Downloaded 11/10/26 12:53 PM UTC

variations. *Water Resour. Res.*, **39**, 1200, https://doi.org/10.1029/2003WR001991.

Zhang, X. B., K. D. Harvey, W. D. Hogg, and T. R. Yuzyk, 2001: Trends in Canadian streamflow. *Water Resour. Res.*, **37**, 987–998, https://doi.org/10.1029/2000WR900357.

——, F. W. Zwiers, G. C. Hegerl, F. H. Lambert, N. P. Gillett, S. Solomon, P. A. Stott, and T. Nozawa, 2007: Detection of human influence on twentieth-century precipitation trends. *Nature*, **448**, 461–465, https://doi.org/10.1038/nature06025.

Zhou, T., I. Haddeland, B. Nijssen, and D. P. Lettenmaier, 2016: Human-induced changes in the global water cycle. *Terrestrial Water Cycle and Climate Change: Natural and Human-Induced Impacts*, *Geophys. Monogr.*, Vol. **221**, Amer. Geophys. Union, 57–69. https://doi.org/10.1002/9781118971772.ch4.

Unauthenticated | Downloaded 11/10/26 12:53 PM UTC